

Simulating the magnetic susceptibility of magnetic nanowire arrays

A. J. Bennett^{a)} and J. M. Xu

Division of Engineering, Box D, Brown University, Providence, Rhode Island 02912

(Received 27 September 2002; accepted 13 March 2003)

We study the magnetostatic interaction and relaxation of nanomagnetic wires in arrays using a Monte-Carlo model. Using this model we describe the magnetic behavior of a two-dimensional array of high aspect ratio ferromagnetic, single-domain nanowires, ordered parallel to one another in a nonmagnetic template. We use this model to determine stable configurations and hysteresis loops, and also investigate the mean field behavior of a typical nanowire array to determine the influence of the geometrical and magnetic parameters on the behavior of the array. © 2003 American Institute of Physics. [DOI: 10.1063/1.1573348]

Magnetic nanostructures are important materials for data storage, but also have potentially equal promise for information processing.¹ Magnetic spin glasses have been studied for their neural network-like properties, and properly designed magnetic nanostructure arrays may exhibit similar effects while being locally controllable.² In view of these important potential applications, we developed a model for investigating the behavior of magnetic nanowire arrays, based on actual structures that can now be routinely grown in our laboratory and an increasing number of others.

The principles of micromagnetics have been established for many years.³ However, analytical solutions to the micromagnetic equations are typically unavailable except for special cases, and full numerical solutions are often time consuming and can only be applied to small systems.⁴ To study the magnetic behavior of larger arrays, appropriate simplifications based on first principles must be made; this is the main goal of this letter.

Template-grown nanostructures are being increasingly recognized as a high-throughput alternative to electron beam lithography, which is time consuming, and limited in both the written area and the minimum feature size. The nanostructures on which we based our model are produced through electrochemical or electroless deposition of metals into long (micron scale) parallel, hexagonal-close-packed pores.⁵ We study nanowires ordered in a two-dimensional hexagonal close-packed array, of diameters 20–100 nm, lattice constants 80–150 nm, and lengths 0.25–100 μm .

In the experimental area, much work on nanomagnetic arrays has met with success. High aspect ratio magnetic nanowires have been grown in disordered anodic oxide templates^{6,7} and in similar templates with hexagonal ordering.^{5,8} Optical interference lithography⁹ and electron beam lithography¹⁰ have also been used to produce lower aspect ratio pillars.

Electron microscopy has shown that electrodeposited nanowires consist of stacked single-crystal regions separated by grain boundaries.¹¹ In such materials, the crystal anisotropy is diminished, and shape anisotropy dominates the preferred axis of magnetization.

Because of shape anisotropy, the magnetization is ori-

ented along the axis of the nanowire, with little deviation from this axis, giving rise to square hysteresis loops.^{11,12} This observation was supported by switching field measurements on individual structures using magnetic force microscopy.⁹ The coercive field of nanowires has been found to decrease as the diameter is reduced, while the remanent magnetization increases.^{6,8} This effect might be used to control the local response of lattice sites in the design of nanomagnetic circuits.

Our system consists of an array of quasio-dimensional, single-domain, vertically oriented, parallel magnetic nanowires. We model this as a hexagonal-close-packed array of parallel, cylindrical ferromagnets of length L , radius r , lattice constant a , and held in place by a nonmagnetic template.

To determine the magnetostatic energy of a two-dimensional array of these nanowires, we begin with the expression for the magnetostatic energy associated with an arbitrary spatial distribution of magnetization^{13,14}

$$E_m = \frac{\mu_0}{4\pi} \int d^3\mathbf{r} \int d^3\mathbf{r}' M_\alpha(\mathbf{r}) M_\beta(\mathbf{r}') \frac{\partial^2}{\partial x_\alpha \partial x'_\beta} \frac{1}{|\mathbf{r} - \mathbf{r}'|}, \quad (1)$$

where α and β stand for the Cartesian indices $\{x, y, z\}$ and \mathbf{M} is the magnetization distribution. Ferromagnetic wires on this size scale should consist of a single magnetic domain, with the magnetization oriented along the long axis of the wire.^{15,16} We therefore make the approximation of axial magnetization, pointing along the z axis.

From Eq. (1), we solved for the total energy change associated with inverting the domain at site i :

$$\Delta E_i = 2(M_0 \pi r^2 L) B p_i - 2\mu_0 \pi (M_0 r^2)^2 \times \sum_{j \neq i} \left(\frac{1}{x_{ij}} - \frac{1}{\sqrt{x_{ij}^2 + L^2}} \right) p_i p_j, \quad (2)$$

where $|p_i| = 1$ is the magnetization direction, x_{ij} is the distance separating lattice sites i and j , M_0 is the saturation magnetization of the wires, and B is the external field. This expression is valid when the magnetization is purely axial, due to shape anisotropy ($L \gg r$).

We solved for the axial component of the stray field to study hysteresis in the system. Close packed wires had a

^{a)}Electronic mail: ajb@brown.edu

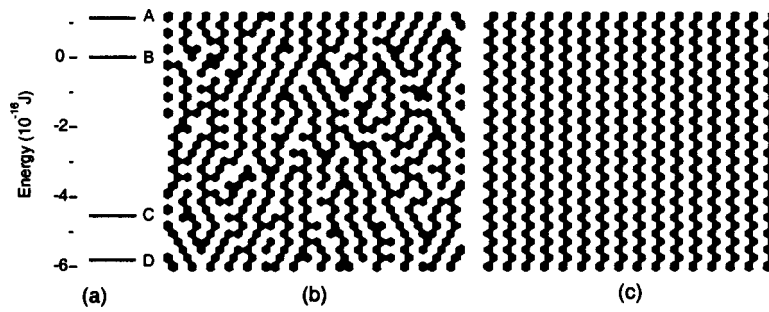


FIG. 1. (a) Energy spectrum of a 32×32 array of nanowires, showing (A) maximum energy (uniform) state (scaled by 0.01), (B) random state, (C) metastable, and (D) ground states. The metastable and random energies were obtained by averaging over 100 different states. (b) Top view of a typical metastable state of the array, showing vertical stripe domains and defects which increase the energy from the zigzag ground state. (c) Top view of the ground state showing ordered zigzag stripe domains.

maximum variation of a few percent in the axial field along the length of the wire, which diminished significantly with separation distance. Therefore, we compared the coercive field H_c to the average axial field to determine whether the nanowire should reverse magnetization. This approximation essentially assumes that an isolated nanowire has a rectangular hysteresis loop; based on the results of micromagnetic nanowire simulations, this assumption appears reasonable.⁷

The average axial (z -directed) field a distance x from a nanowire is

$$\langle H_z(z,x) \rangle_z = \frac{-M_0 \pi r^2}{2L} \left(\frac{1}{x} - \frac{1}{\sqrt{x^2 + L^2}} \right). \quad (3)$$

The pairwise interaction energy is equal to $2\mu_0 M_0 \pi r^2 L \langle H_z(z,x) \rangle$, which is the sum of the stray field from site i , times the volume of nanowire j and vice versa. The negative stray fields of dipolar nanowires favor antiferromagnetic ordering in the array.

Using a Monte-Carlo method, we probed the stable states of the system, and investigated how the susceptibility of the system depended on the parameter values used.^{17,18}

The hexagonal-close-packed lattice is obtained from the square lattice by offsetting alternating rows by half a lattice constant and scaling the row spacing by a factor of $2/3\sqrt{3}$; when this transformation is applied to the checkerboard ground state of the square lattice it yields zigzag stripes.¹⁹ Our observations suggest that the antiferromagnetic ground state in a two-dimensional hexagonal lattice does correspond to vertical, zigzag stripes.

The energy spectrum of configurations at zero temperature, a typical metastable state, and the ground state, are shown in Fig. 1; these results confirm that the Monte-Carlo method works. The metastable state differs from the ground state due to the lateral disorder, and resembles images of frustrated nanowire arrays obtained by magnetic force microscopy.⁸ These observations are also reminiscent of frustration in spin glasses and other magnetic systems with memory.²

The collective or mean field magnetic behavior of a material is partly described by its hysteresis loop. In our model array, the interactions give rise to an overall hysteresis loop which is quite different from a simple superposition of the hysteresis loops of the individual elements.⁷ The hysteresis loop is a plot of the normalized system magnetization, defined as $m = (N_\uparrow - N_\downarrow) / (N_\uparrow + N_\downarrow)$. In other words, m is the

mean field average of p_i . To generate these loops, we started at a high external field value, B_0 , with a completely polarized stable state ($m = 1$). The field was swept to $-B_0$ and back to B_0 .

For small values of H_c the hysteresis loop has a thin sigmoid shape due to the magnetostatic interaction. A finite value of H_c separates the edges of the hysteresis loop but does not otherwise change the shape of the curve. In this model the H_c and stray fields are independent.

Figure 2(a) depicts the hysteresis loops for different values of the individual wire coercivity, H_c , revealing broadening of the loops as H_c is increased. The slope of the hysteresis loop edges increases as L is increased, as shown in Fig. 2(b). For shorter wire lengths, the hysteresis loop widens at small applied fields. Long wires have an interaction energy proportional to $1/x$ which is long ranged and less likely to result in frustration, while shorter wires have a $1/x^3$ interaction which decays more rapidly, making frustration more likely.

From the equations, the linear magnetic susceptibility χ_M , or slope, of the array can be estimated using a simple mean field method based on the magnetostatic interactions. This calculation allowed us to determine how the structural and material parameters influenced the shape of the hysteresis loops, and thereby the energy cost of making the transition from one global state to another.

We replace the interaction term in the inversion energy

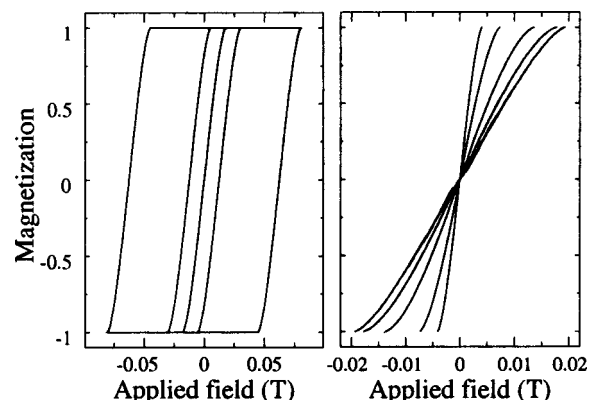


FIG. 2. (a) Hysteresis loops for three values of H_c (0 , 10^4 , and $5 \times 10^4 \text{ A m}^{-1}$). The loop is broadened due to increasing H_c , but the shapes of the loop edges are unchanged. (b) A family of hysteresis loops at $H_c = 0$, for several different values of L . The curve with smallest slope has L of 500 nm , and the slope increases as L is increased to 1000 , 2000 , 5000 , and 10000 nm .

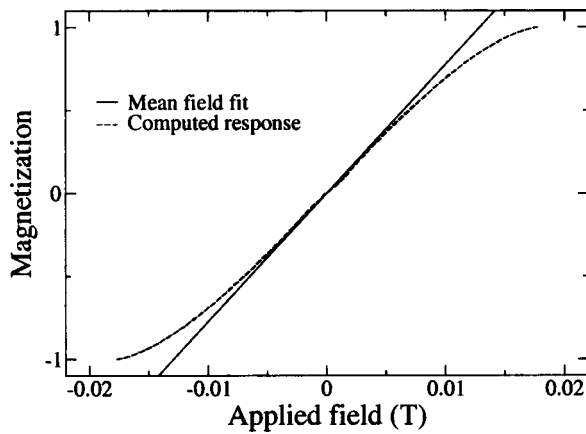


FIG. 3. Hysteresis loop of magnetic nanoarray for $H_c=0$, with mean-field theory fit to the curve. The mean field theory describes a spatially averaged environment, with equal populations of spatially dispersed up and down magnetizations. This works for small magnetizations, when the normalized magnetization is much larger than zero, the approximation breaks down.

with an averaged interaction that depends only on the average magnetization of the array. This averaged interaction, denoted by K , is a constant for a specified array size N , lattice constant a , and lattice type.

Operating under the Monte-Carlo dynamics, the system evolves to a stable state, for which $\Delta E_i \geq 0$ for all i . Therefore, $\Delta E_i = 0$ represents the boundary of the region in state space which consists of stable states. Relating the set of stable states to the dipole moments of the lattice sites is an important basis for designing memories and other devices based on these systems.^{2,20}

We estimate the stable value of m for different values of B by setting $\Delta E_i = 0$ and solving for m . We also replace B with $B - H_c/\mu_0$ to account for the offset due to the finite coercivity. This gives a linear equation for m , and shows how parameter changes influence the shape of the hysteresis loop

$$m = \left(\frac{1}{2\pi N K \mu_0} \right) \left(\frac{L}{M_0 r^2} \right) \left(B - \frac{H_c}{\mu_0} \right). \quad (4)$$

This equation describes the macroscopic behavior of the system for low applied field, under the assumption that the two terms in Eq. (2)—the external field energy and the internal interaction energy—are equal and opposite when the system is in a low-field stable state. For a weakly magnetized system ($m \ll 1$) the up- and down-oriented lattice sites are intermixed and so the parameter K , applies equally well to both orientations. At higher polarization, the average separation distance between one orientation grows larger as their number diminishes, while the opposite occurs for the other orientation. The single parameter K cannot describe this behavior and the approximation breaks down (see Fig. 3). However, at higher fields the equation still captures the dependence of the hysteresis loop on the geometrical and magnetic parameters of the array.

We can now use these results to explore the behavior of this system for a range of system parameters. We found an analytical relationship between the parameters of the array and the shape of the hysteresis loops based on a simple mean field model valid for low applied field. Simulations incorporating temperature dependence and crystal anisotropy can also build on these results in further studies of the array properties.

The collective behavior of these arrays is reminiscent of neural networks and spin glasses. However, nanostructure arrays are more controllable than atomic spin glasses because they can be designed specifically to control the interactions between lattice sites of variable dipole strength. The findings presented here could help guide the design of such arrays. The magnetic response of a small array of these structures behaves like a model neuron, and collective behavior in an inhomogeneously structured cluster of interacting magnetic arrays may potentially be used for computation. More specifically, it might be possible to fabricate a Hopfield network out of such systems.²⁰ This is an ongoing area of research that we hope will benefit from findings like those presented earlier.

This work was supported by DARPA and NSF.

¹P. R. Kotiuga and T. Toffoli, *Physica D* **120**, 139 (1998).

²D. J. Amit, H. Gutfreund, and H. Sompolinski, *Phys. Rev. A* **32**, 1007 (1985).

³W. F. Brown, *Micromagnetics* (Interscience, New York, 1963).

⁴R. Hertel, *J. Appl. Phys.* **90**, 5752 (2001).

⁵A. J. Yin, J. Li, W. Jian, A. J. Bennett, and J. M. Xu, *Appl. Phys. Lett.* **79**, 1039 (2001).

⁶L. Cheng-Zhang and J. C. Lodder, *J. Magn. Magn. Mater.* **88**, 236 (1990).

⁷V. Raposo, J. M. Garcia, J. M. González, and M. Vázquez, *J. Magn. Magn. Mater.* **222**, 227 (2000).

⁸K. Nielsch, R. B. Wehrspohn, J. Barthel, J. Kirschner, and U. Gösele, *Appl. Phys. Lett.* **79**, 1360 (2001).

⁹M. C. Abraham, H. Schmidt, T. A. Savas, H. I. Smith, C. A. Ross, and R. J. Ram, *J. Appl. Phys.* **89**, 5667 (2001).

¹⁰C. A. Ross, H. I. Smith, T. Savas, M. Schattenburg, M. Farhoud, M. Hwang, M. Walsh, M. C. Abraham, and R. J. Ram, *J. Vac. Sci. Technol. B* **17**, 3168 (1999).

¹¹Y. Peng, H.-L. Zhang, S.-L. Pan, and H.-H. Lin, *J. Appl. Phys.* **87**, 7405 (2000).

¹²K. Ounadjela, R. Ferré, L. Louail, J. M. George, J. L. Maurice, L. Piroux, and S. Dubois, *J. Appl. Phys.* **81**, 5455 (1997).

¹³K. Y. Guslienko, *Appl. Phys. Lett.* **75**, 394 (1998).

¹⁴A. Hubert and R. Schäfer, *Magnetic Domains: The Analysis of Magnetic Microstructures* (Springer, Berlin, 1998).

¹⁵C. Kittel, *Phys. Rev.* **70**, 965 (1946).

¹⁶C. Kittel, *Phys. Rev.* **21**, 541 (1949).

¹⁷J. M. Thijssen, *Computational Physics* (Cambridge University Press, Cambridge, 1999).

¹⁸R. J. Glauber, *J. Math. Phys.* **4**, 294 (1963).

¹⁹T. Aign, P. Meyer, S. Lemerle, J. P. Jamet, J. Ferré, V. Mathet, C. Chepert, J. Gierak, C. Vieu, F. Rousseaux, H. Launois, and H. Bermas, *Phys. Rev. Lett.* **81**, 5656 (1998).

²⁰J. J. Hopfield, *Proc. Natl. Acad. Sci. U.S.A.* **79**, 2554 (1982).